Electronic Supporting Information

Low band gap diketopyrrolopyrrole-based small molecule bulk heterojunction solar cells: Influence of terminal side chain on morphology and photovoltaic performance

Quoc-Viet Hoang,[a,b] Chang Eun Song,[a,b] In-Nam Kang,[c] Sang-Jin Moon,[a,b] Sang Kyu Lee,[a,b] Jong-Cheol Lee,[a,b] and Won Suk Shin [a,b,*]

[a] *Energy Materials Research Center, Korean Research Institue of Chemical Technology (KRICT), 141 Gajeong-ro, Yuseong-gu, Daejeon, 305-600, Korea; Email: shinws@krict.re.kr*

[b] *Department of Nanomaterials Science and Engineering, University of Science & Technology (UST), 217 Gajeong-ro, Yuseong-gu, Daejeon, 305-350, Korea*

[c] *Department of Chemistry, The Catholic University of Korea, Gyeonggido 90-2, Korea*

Table of Contents

General

NMR: ^{1}H and ^{13}C nuclear magnetic resonance (NMR) spectroscopy spectra were recorded on Bruker DRX-300 FT-NMR and Bruker Avance-500 MHz spectrometer at 25 ^{o}C unless otherwise noted. ^{1}H and ^{13}C NMR spectra are referenced to Me_4Si using the residual solvent peak impurity of the given solvent. Chemical shifts are reported in ppm and coupling constants in Hz as absolute values.

UV-vis: UV-visible spectroscopies were recorded using wither a Shimadzu UV-2550 spectrophotometer at room temperature unless otherwise noted. All solution UV-vis experiments were run in $CHCl_3$. Films were prepared by spin-coating $CHCl_3$ solutions onto quartz substrates.

CHNS: Combustion analyses were performed by the MSI analytical lab at the Analytical Center, Korea Research Institute of Chemical Technology.

Mass Spectrometry: Full scan, low resolution and MALDI-TOF mass spectrometry was carried out at the Analytical Center, Korea Research Institute of Chemical Technology.

DSC and TGA: Differential scanning calorimetry (DSC) was determined using a TA Instruments DSC (Model Q-1000) with about 5 mg samples at a rate of 10 °C/ min in the temperature range of 0 to 350 °C, unless otherwise stated. Thermogravemetric analysis (TGA) was carried out at the Analytical Center, Korea Research Institute of Chemical Technology. Samples were run under N_2 and heated from room temperature to 600 °C at a rate of 20 °C/ min.

Electrochemistry: All electrochemical measurements were performed using IVIUMSTAT instrument model PV-08 in a standard three-electrode, one compartment configuration equipped with $Ag/AgNO_3$ electrode, Pt wire and Pt electrode (dia. 1.6 mm), as the pseudo reference, counter electrode and working electrode, respectively. Pt working electrodes were polished with alumina. 0.1 M tetrabutyl ammonium hexafluorophosphate in anhydrous acetonitrile as supporting electrolyte. The experiments were purged with argon and then carried at a scan rate of 20 mV s^{-1}. SMs thin films were prepared by drop casting onto the Pt working electrode from chloroform solution and dried before measurements. The electrochemical onsets were determined at the position where the current starts to differ from the baseline. The potential of the

$Ag/AgNO_3$ reference electrode was calibrated by using the ferrocene/ferrocenium redox couple (Fc/Fc^+), which has a known reduction potential of −4.8 eV. The highest occupied molecular orbital (HOMO) of copolymers were calculated from the onset oxidation potentials ($E_{oxonset}$) according to: HOMO= $-(E_{oxonset} + 4.8)$ (eV). The lowest unoccupied molecular orbital (LUMO) of copolymers were calculated from the onset reduction potentials ($E_{redonset}$) according to: LUMO= $-(E_{redonset} + 4.8)$ (eV).

TEM characterization: The active layers (SMs:$PC_{71}BM$) were spin-coated onto Glass/ITO/PEDOT:PSS. After drying, the samples were dipped in water and thin films were collected and transferred to Cu grids. Bright-field (BF) TEM images of samples were obtained at 200 kV under low dose conditions with TECVAIG^2 – T – 20S electron microscope. Each sample was characterized several images (at least 6 images) over 2-3 sections per grid to ensure that analysis was based on a representative region of the sample.

SCLC devices' fabrication and testing: Mobility measurements of SM/$PC_{71}BM$ (w/w, 1:1) with and without CN were done by a charge-only space-charge limited current (SCLC) method with the following diode structures: ITO/PEDOT:PSS/active layer/Au for hole and Al/active layer/Al for electron by taking current-voltage current in the range 0–7 V and fitting the results to a space-charge limited form. The charge carrier mobilities were calculated using the SCLC model, where the SCLC is described by $J = 9\varepsilon_0\varepsilon_r\mu V^2/8L^3$, where J is the current density, L is the film thickness of the active layer, μ is the hole or electron mobility, ε_r is the relative dielectric constant of the transport medium, ε_0 is the permittivity of free space (8.85×10^{-12} F m^{-1}), V is the internal voltage in the device, and $V = V_{appl} - V_r - V_{bi}$, where V_{appl} is the applied voltage to the device, V_r is the voltage drop due to contact resistance and series resistance across the electrodes, and V_{bi} is the built-in voltage due to the relative work function difference of the two electrodes.

Fabrication of the organic field effect transistors (OFETs): OFET devices were fabricated in a bottom-contact geometry (channel length = 12 μm, width = 120 μm). The source and drain contacts consisted of gold (100 nm), and the dielectric was silicon oxide (SiO_2) with a thickness of 300 nm. The SiO_2 surface was cleaned, dried, and pretreated with a solution of 1.0 mM octyltrichlorosilane (OTS-8) in toluene at room temperature for 2 h under nitrogen to produce nonpolar and smooth surfaces onto which the polymers could be spin-coated. The polymers were dissolved to a concentration of 0.5 wt% in chloroform. Films of the organic semiconductors were spin-coated at 1000 rpm for 50 s to a thickness of 50 nm, followed by an annealing process. All device fabrication procedures and measurements were carried out in air at room temperature. The FET characteristics were determined under ambient conditions, and no precautions were taken to insulate the materials and devices from exposure to air, moisture, or light. The field effect mobility was calculated according to the following equation: Saturated regime ($V_D > V_G$): $I_D = (W/2L)\mu C_i(V_G - V_T)^2$, where I_D is the drain current in the saturated regime, W and L are the channel width and length, respectively, μ is the field effect mobility, C_i is the capacitance per unit area of the gate dielectric layer, and V_G and V_T are the gate and threshold voltages, respectively.

Material Syntheses

2,2′-Bithiophene-5-boronic acid pinacol ester and 5-hexyl-2,2′-bithiophene-5′-boronic acid pinacol ester were purchased from Sigma-Aldrich Chemical Co. and used as received. Other chemicals and solvents were used as received from commercial sources without further purification. Tetrahydrofuran (THF) was distilled over sodium/benzophenone. 3,6-Bis(5-bromothienyl)-2,5-di(2-ethylhexyl) pyrrolo[3,4-c]pyrrolo-1,4-dione (1) and 2,6-bis(trimethyltin)-4,8-bis(5-(2-ethylhexyl)thiophen-2-yl)benzo [1,2-*b*:4,5-*b*′]dithiophene (3) were synthesized following the previously published procedure.[1, 2]

3-[5-(5-hexyl-2,2’-bithiophen-5’-yl)thiophen-2-yl]-6-(5-bromothiophen-2-yl)-2,5-di(2-ethylhexyl) pyrrolo[3,4-c]pyrrolo-1,4-dione (2a).

A mixture of 5-hexyl-2,2′-bithiophene-5′-boronic acid pinacol ester (1.45 g, 3.84 mmol), 3,6-bis(5-bromothienyl)-2,5-di(2-ethylhexyl) pyrrolo[3,4-c]pyrrolo-1,4-dione (1) and 1M sodium carbonate (15 mL) was added into 2-neck round bottom flask contained 100 mL of toluene. The mixture was degassed and followed by adding of aliquat 336 (3 drops) and tetrakis(triphenylphosphine) palladium(0) (0.11 g, 0.095 mmol). The reaction mixture was degassed again and stirred at 90^{o}C for 24 h under Argon atmosphere. The mixture was then loaded onto silica, slurried in methanol, filtered and purified by flash chromatography using a hexanes/chloroform (1 : 1) gradient. After fraction collection and solvent removal, a deep blue solid was obtained. This crude product was slurried in methanol (300 mL), sonicated for 10 minutes and filtered.

The solid was washed with excess methanol and then dried under vacuum at 50°C for 24 hours. 1.01 g of deep blue solid was collected (31% yield). ^{1}H NMR (300 MHz,CDCl$_3$): δ (ppm) 8.97 (d, J = 4.2 Hz, 1H); 8.62 (d, J = 4.2 Hz, 1H); 7.28 (d, J=4.2, 1H); 7.21 (d, J = 4.2 Hz, 2H); 7.04 (t, J=4.2 Hz, 2H); 6.71 (d, J=4.2, 1H); 4.06-3.92 (m, 4H); 2.80 (t, J=7.6, 2H); 1.88 (m, 2H); 1.69 (m, 2H); 1.33 (m, 22H); 0.88 (m, 15H). ^{13}C NMR (125 MHz, CDCl$_3$): δ (ppm) 161.82; 161.42; 146.66; 143.27; 140.55; 139.28; 138.28; 137.41; 135.03; 134.11; 134.05; 131.53; 131.50; 127.80; 126.10; 125.19; 124.57; 124.19; 123.97; 118.51; 108.55; 108.02; 46.14; 39.40; 39.28; 31.70; 31.67; 30.51; 30.37; 28.90; 28.70; 28.48; 23.83; 23.73; 23.26; 23.19; 22.71; 14.23; 14.21; 14.16; 10.69; 10.64. EI-MS m/z calcd for $C_{44}H_{55}BrN_2O_2S_4$ (M^+): 850.23; found: 851

3-[5-(2,2'-bithiophen-5-yl)thiophen-2-yl]-6-(5-bromothiophen-2-yl)-2,5-di(2-ethylhexyl) pyrrolo[3,4-c]pyrrolo-1,4-dione (2b).

The procedure for the synthesis of (2b) was followed using 2,2′-bithiophene-5-boronic acid pinacol ester (1.12 g, 3.84 mmol) instead of 5-hexyl-2,2′-bithiophene-5′-boronic acid pinacol ester to obtain 1.05 g of deep blue solid (36% yield). ^{1}H NMR (300 MHz,CDCl$_3$): δ (ppm) 8.96 (d, J = 4.2 Hz, 1H); 8.63 (d, J = 4.1 Hz, 1H); 7.30 (d, J = 4.1 Hz, 1H); 7.28-7.20 (m, 4H); 7.11 (d, J = 3.7 Hz, 1H); 7.05 (dd, J^1 = 3.6 Hz, J^2 = 1.4 Hz, 1H); 4.06-3.93 (m, 4H); 1.88 (m, 2H); 1.31 (m, 16H); 0.88 (m, 12H). ^{13}C NMR (125 MHz, CDCl$_3$): δ (ppm) 161.77, 161.41, 142.95, 140.42, 138.55, 138.41, 137.30, 136.76, 135.11, 134.78, 131.50, 128.19, 128.03, 126.06, 125.32, 124.75, 124.41, 118.60, 108.51, 108.10, 46.13, 39.40, 39.26, 30.51, 30.33, 28.70, 28.48, 23.83, 23.73, 23.26, 23.18, 14.23, 14.16, 10.69, 10. 64. EI-MS m/z calcd for $C_{38}H_{43}BrN_2O_2S_4$ (M^+): 766.14; found: 767

2,6-bis{5-{6-[5-(5-hexyl-2,2'-bithiophen-5'-yl)thiophen-2-yl]-2,5-di(2-ethylhexyl)pyrrolo[3,4-c]pyrrolo-1,4-dione-3-yl}thiophen-2-yl}-4,8-bis(5-(2-ethylhexyl)thiophen-2-yl)benzo[1,2-*b*:4,5-*b′*]dithiophene (BDT(DPP-TTHex)$_2$).

50 mL sealed tube was charged with 2a (665 mg, 0.78 mmol), 3 (329 mg, 0.363 mmol) and anhydrous toluene/DMF (20 mL/2 mL). The mixture was degassed and followed by adding of tetrakis(triphenylphosphine) palladium(0) (21 mg, 5% mmol). The reaction mixture was degassed again and stirred at 100°C for 24 h under Argon atmosphere. The mixture was then slurried in methanol, filtered

and purified by flash chromatography using a hexanes/chloroform gradient from 1/2 (to remove starting materials and impurities) to 1/10 (to collect product). After fraction collection and solvent removal, a deep green solid was obtained. This crude product was slurried in methanol (300 mL), sonicated for 10 minutes and filtered. The solid was washed with excess hot methanol, acetone, hexanes and then dried under vacuum at 50°C for 24 hours. 562 mg of deep green solid was collected (76% yield). ^{1}H NMR (500 MHz, $CDCl_3$): δ (ppm) 9.03 (m, 4H); 7.51 (s, 2H); 7.43 (m, 2H); 7.14 (m, 2H); 7.06 (m, 2H); 7.01 (m, 2H); 6.94 (m, 2H); 6.89 (m, 2H); 6.81 (m, 2H); 6.61 (m, 2H); 3.91 (broad, 8H); 2.99 (d, J=6.3, 4H); 2.71 (t, J=6.9, 4H); 1.87 (m, 6H); 1.68-1.20 (broad, 64H); 1.10-0.82 (m, 42H). ^{13}C NMR (125 MHz, $CDCl_3$): δ (ppm) 161.11; 161.06; 146.14; 146.09; 142.41; 141.56; 138.75; 138.68; 138.55; 138.18; 137.17; 136.81; 136.56; 136.51; 134.06; 133.95; 128.60; 128.08; 127.54; 125.44; 125.31; 124.77; 123.88; 123.61; 123.36; 123.23; 119.96; 119.93; 108.20; 107.95; 45.95; 45.77; 41.32; 39.42; 34.53; 32.70; 31.56; 31.37; 30.36; 30.16; 29.00; 28.87; 28.58; 28.47; 25.72; 23.61; 23.26; 23.22; 23.16; 22.60; 14.25; 14.19; 14.17; 14.07; 10.88; 10.61; 10.52. Anal. Calcd. for $C_{122}H_{150}N_4O_4S_{12}$: C, 69.08; H, 7.13; N, 2.64; S, 18.14. Found: C, 68.96; H, 7.12; N, 2.65; S, 18.05%. MS (MALDI-TOF) m/z calcd for $C_{122}H_{150}N_4O_4S_{12}$ (M^+): 2119.83; found: 2121.

2,6-bis{5-{6-[5-(2,2'-bithiophen-5-yl)thiophen-2-yl]-2,5-di(2-ethylhexyl)pyrrolo[3,4-c]pyrrolo-1,4-dione-3-yl}thiophen-2-yl}-4,8-bis(5-(2-ethylhexyl)thiophen-2-yl)benzo[1,2-*b*:4,5-*b′*]dithiophene ($BDT(DPP-TT)_2$).

The procedure for the synthesis of $BDT(DPP-TT)_2$ was followed using 3-[5-(2,2'-bithiophen-5-yl)thiophen-2-yl]-6-(5-bromothiophen-2-yl)-2,5-di(2-ethylhexyl) pyrrolo[3,4-c]pyrrolo-1,4-dione (2b) (600 mg, 0.78 mmol) instead of 3-[5-(5-hexyl-2,2'-bithiophen-5'-yl)thiophen-2-yl]-6-(5-bromothiophen-2-yl)-2,5-di(2-ethylhexyl) pyrrolo[3,4-c]pyrrolo-1,4-dione (2a) to obtain 520 mg of deep green solid (73% yield). ^{1}H NMR (500 MHz, $CDCl_3$): δ (ppm) 9.05 (d, J=4.2, 2H); 9.00 (d, J=4.2, 2H); 7.53 (s, 2H); 7.42 (d, J=3.1, 2H); 7.17 (m, 4H); 7.10 (m, 4H); 6.96 (m, 8H); 3.94 (m, 8H); 2.99 (d, J=6.3, 4H); 1.88 (m, 6H); 1.59-1.20 (broad, 48H); 1.10-0.81 (m, 36H). ^{13}C NMR (125 MHz, $CDCl_3$): δ (ppm) 161.10; 146.13; 142.13; 141.71; 138.71; 138.38; 137.85; 137.18; 137.06; 136.91; 136.73; 136.55; 134.64; 128.61; 128.09; 127.90; 127.80; 125.46; 125.33; 124.84; 124.22; 124.09; 123.89; 123.27; 120.04; 108.19; 108.07; 45.96; 45.79; 41.34; 39.44; 34.53;

32.70; 30.38; 29.01; 28.61; 28.48; 25.73; 23.64; 23.26; 23.23; 23.16; 14.26; 14.20; 14.17; 10.89; 10.62; 10.54. Anal. Calcd. for $C_{110}H_{126}N_4O_4S_{12}$: C, 67.65; H, 6.50; N, 2.87; S, 19.70. Found: C, 67.60; H, 6.51; N, 2.79; S, 19.66%. MS (MALDI-TOF) m/z calcd for $C_{110}H_{126}N_4O_4S_{12}$ (M^+): 1951.65; found: 1953.

Table S1. Optical data of the SM BDT(DPP-TT)$_2$ and BDT(DPP-TTHex)$_2$

Compound	Solution			Film		
	λ_{max}	λ_{onset}	$E_g^{opt}(s)$	λ_{max}	λ_{onset}	$E_g^{opt}(f)$
DBT(DPP-TTHex)$_2$	680	727	1.71	750	830	1.49
DBT(DPP-TT)$_2$	677	721	1.72	744	810	1.53

s: solution, f : film

Table S2. Hole Mobility and Electron Mobility of SM BDT(DPP-TTHex)$_2$ and BDT(DPP-TT)$_2$

Active layer	R_{sh} [Ω cm^2]	R_s [Ω cm^2]	μ_h [cm^2/V s] [a)]	μ_e [cm^2/V s] [b)]
BDT(DPP-TTHex)$_2$: PC$_{71}$BM	7.3X10^3	2.90	1.54 X 10^{-4}	7.22 X 10^{-8}
BDT(DPP-TTHex)$_2$: PC$_{71}$BM+ 0.5%CN	1.2X10^4	3.82	1.01 X 10^{-5}	2.39 X 10^{-5}
BDT(DPP-TT)$_2$: PC$_{71}$BM	1.2X10^4	3.82	2.88 X 10^{-4}	5.71 X 10^{-5}
BDT(DPP-TT)$_2$: PC$_{71}$BM+ 0.3%CN	3.8X10^4	2.28	1.28 X 10^{-5}	5.46 X 10^{-5}

[a)] Hole-only devices : ITO/ PEDOT:PSS (40 nm)/Active layer (~90 nm)/Au (100 nm)

[b)] Electron-only devices : Al (100 nm)/Active layer (~90 nm)/Al (100 nm)

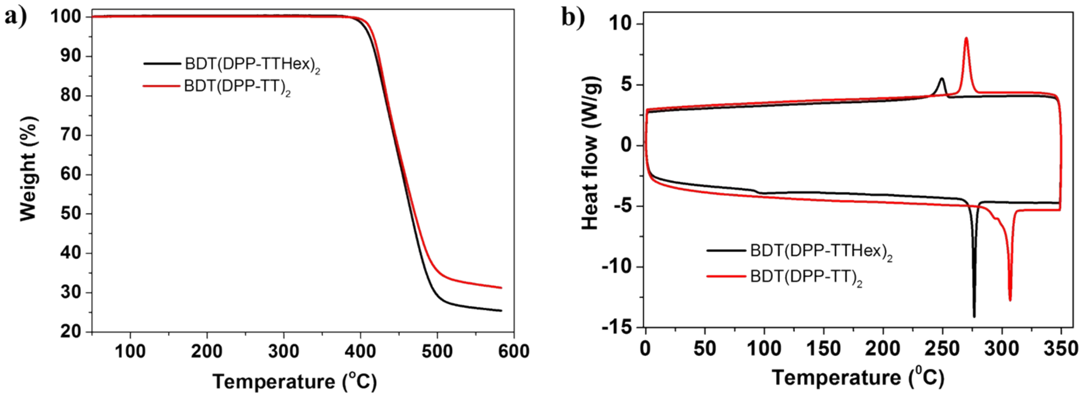

Fig. S1 **a)** Thermogravimetric analysis (TGA) of Compounds BDT(DPP-TTHex)$_2$ and BDT(DPP-TT)$_2$ from room temperature to 600°C at 20°C / min. **b)** DSC scan of BDT(DPP-TTHex)$_2$ and BDT(DPP-TT)$_2$ from 0°C to 350°C at 10°C/min.

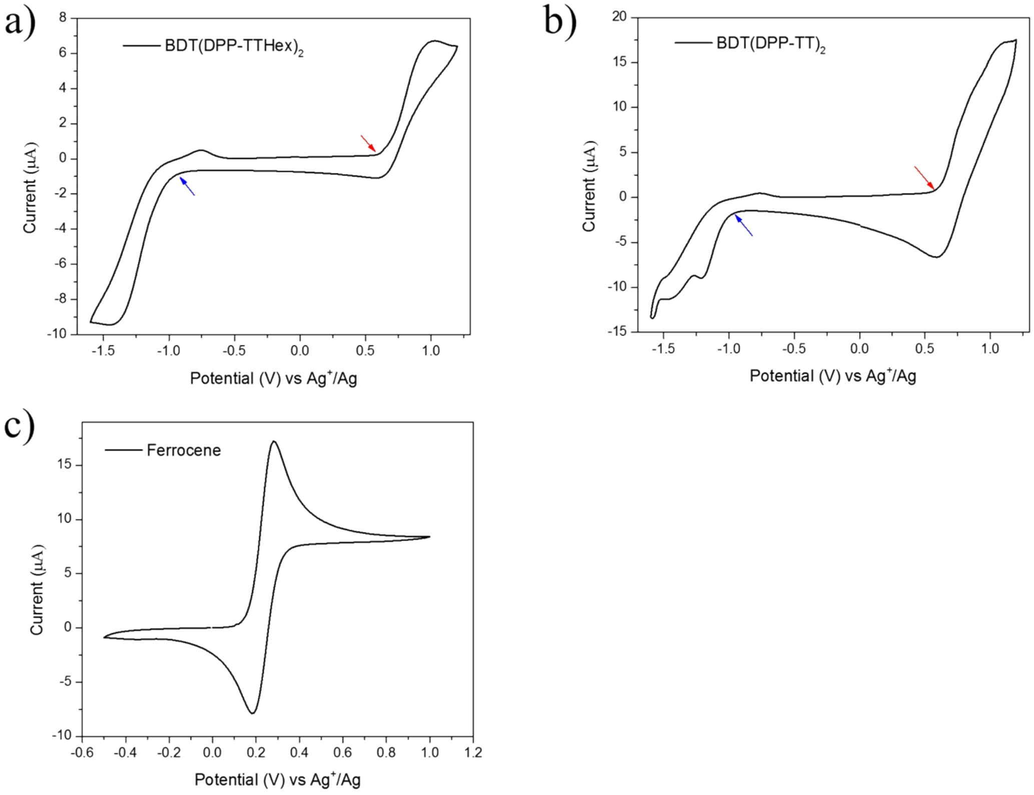

Fig. S2 Cyclic Voltammetry of BDT(DPP-TTHex)$_2$ and BDT(DPP-TT)$_2$ and ferrocene as standard

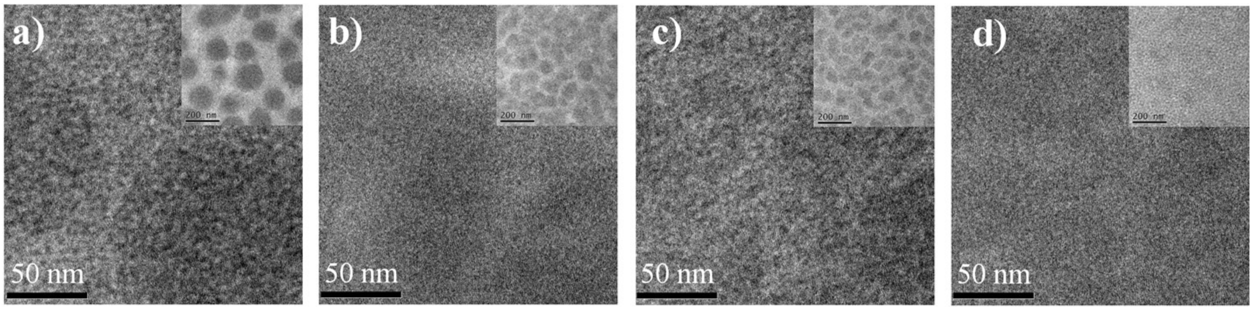

Fig. S3 TEM images of BDT(DPP-TTHex)$_2$: PC$_{71}$BM 1:1 a) without and b) with 0.5% CN. BDT(DPP-TT)$_2$: PC$_{71}$BM 1:1 c)without and d)with 0.3% CN (fibril feature)

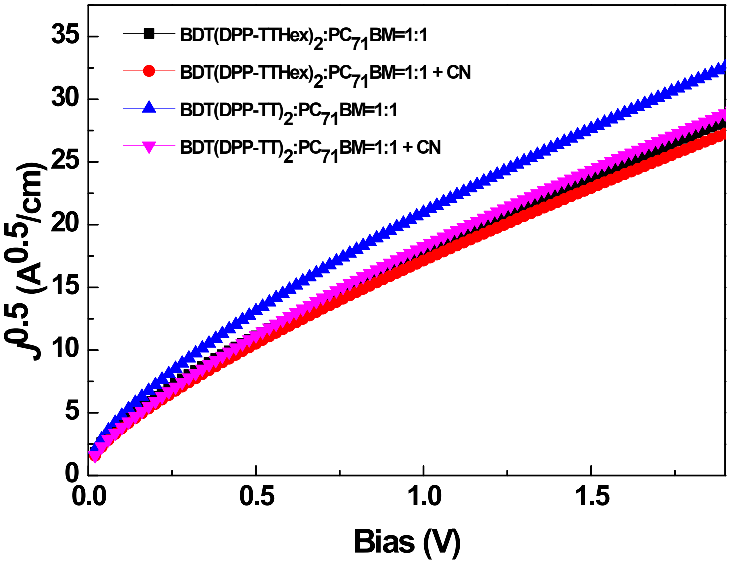

Fig. S4 Space Charge Limited Current (SCLC) for Hole Mobility of Compounds BDT(DPP-TTHex)$_2$ and BDT(DPP-TT)$_2$

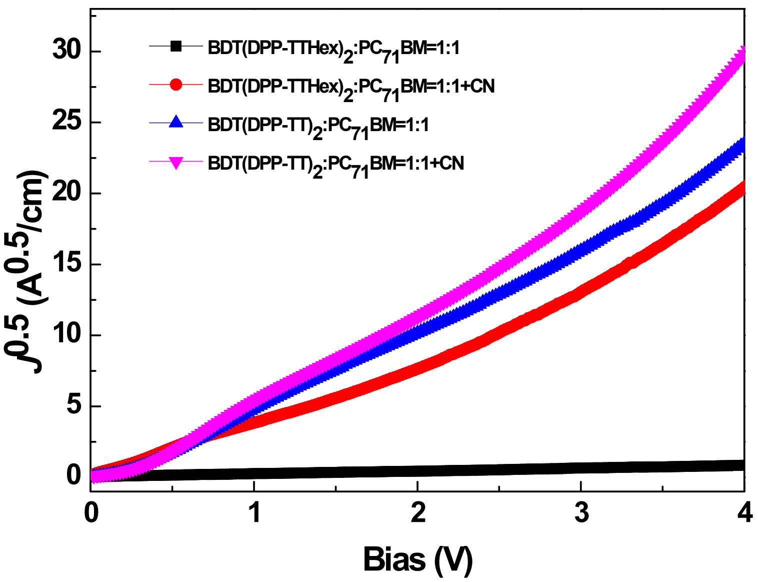

Fig. S5 Space Charge Limited Current (SCLC) for Electron Mobility of Compounds BDT(DPP-TTHex)$_2$ and BDT(DPP-TT)$_2$

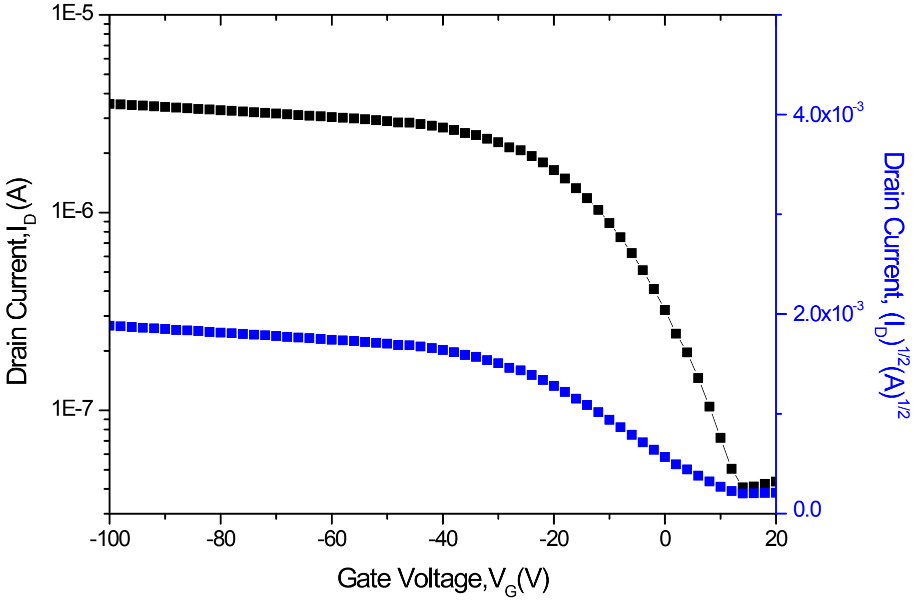

Fig. S6 Performance of the OFET based on pristine BDT(DPP-TTHex)$_2$ (p-type, V_{ds}= -80V). μ_h= 2.2 x 10^{-2} cm^{2}V^{-1}s^{-1}

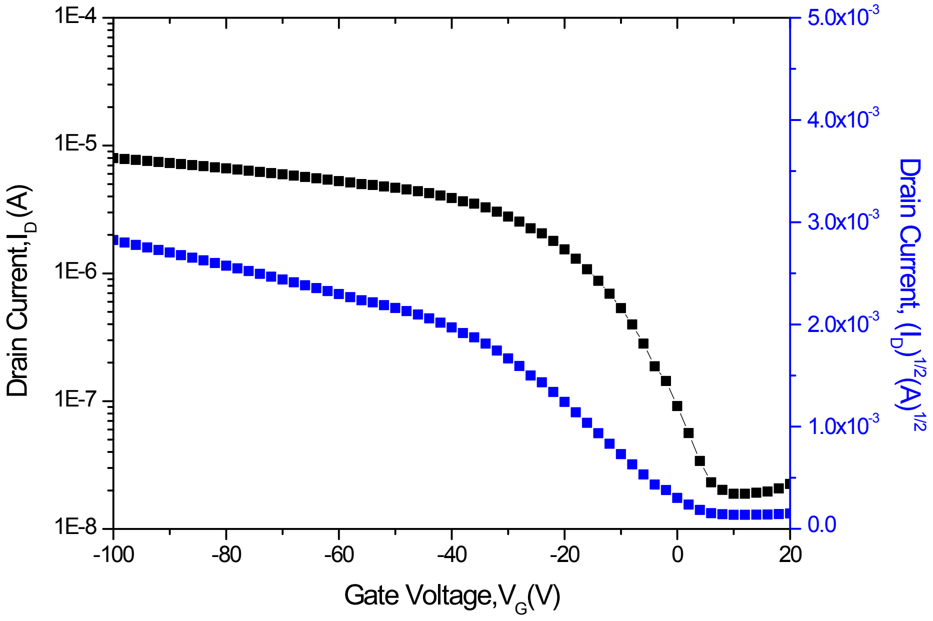

Fig. S7 Performance of the OFET based on pristine BDT(DPP-TT)$_2$ (p-type, V_{ds}= -80V). μ_h= 2.1 x 10^{-2} cm^{2}V^{-1}s^{-1}

^{1}H NMR and ^{13}C NMR Spectra of Compounds

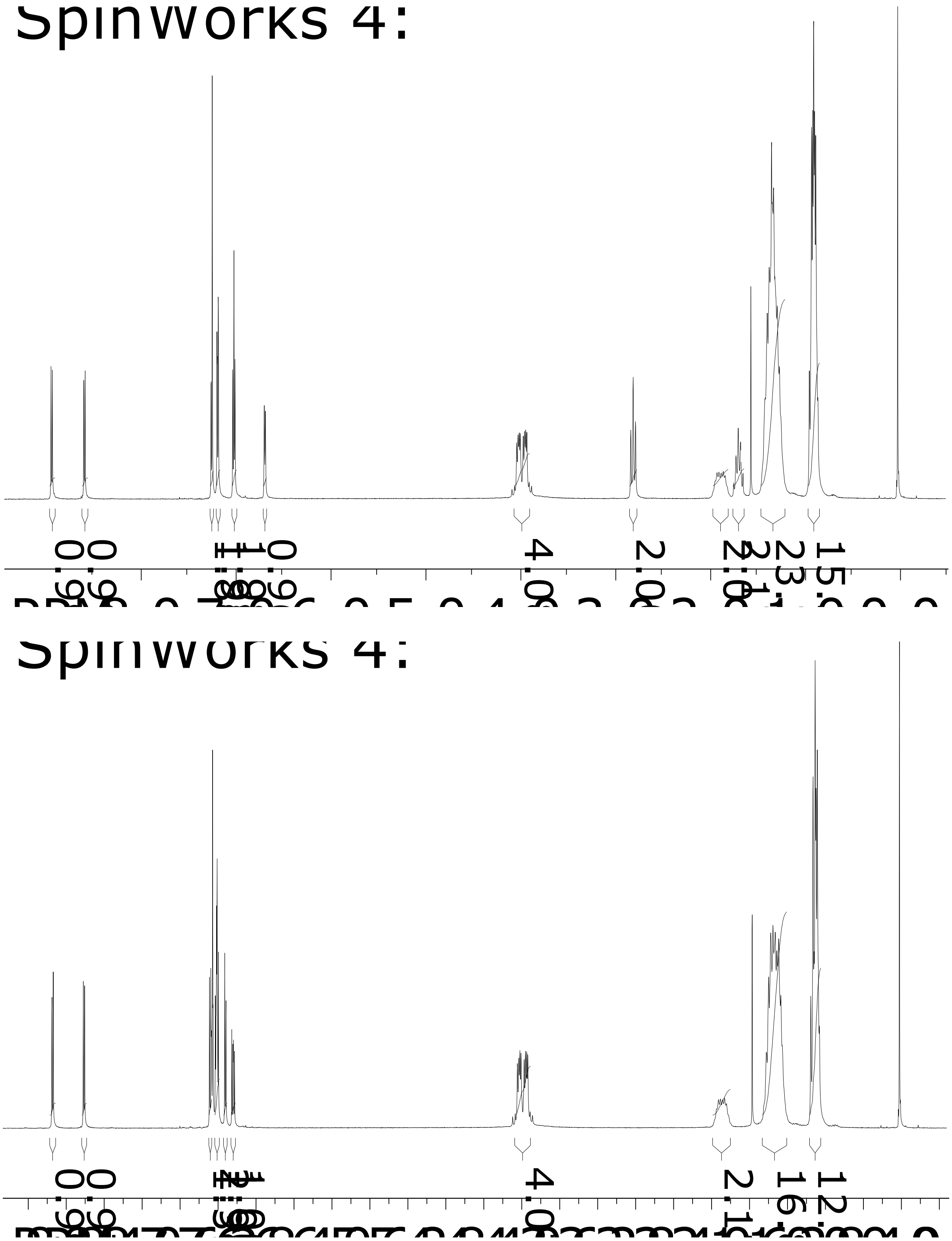

^{1}H NMR spectrum of compound **2a** (top) and **2b** (bottom) in $CDCl_3$ (δ 7.26 ppm).

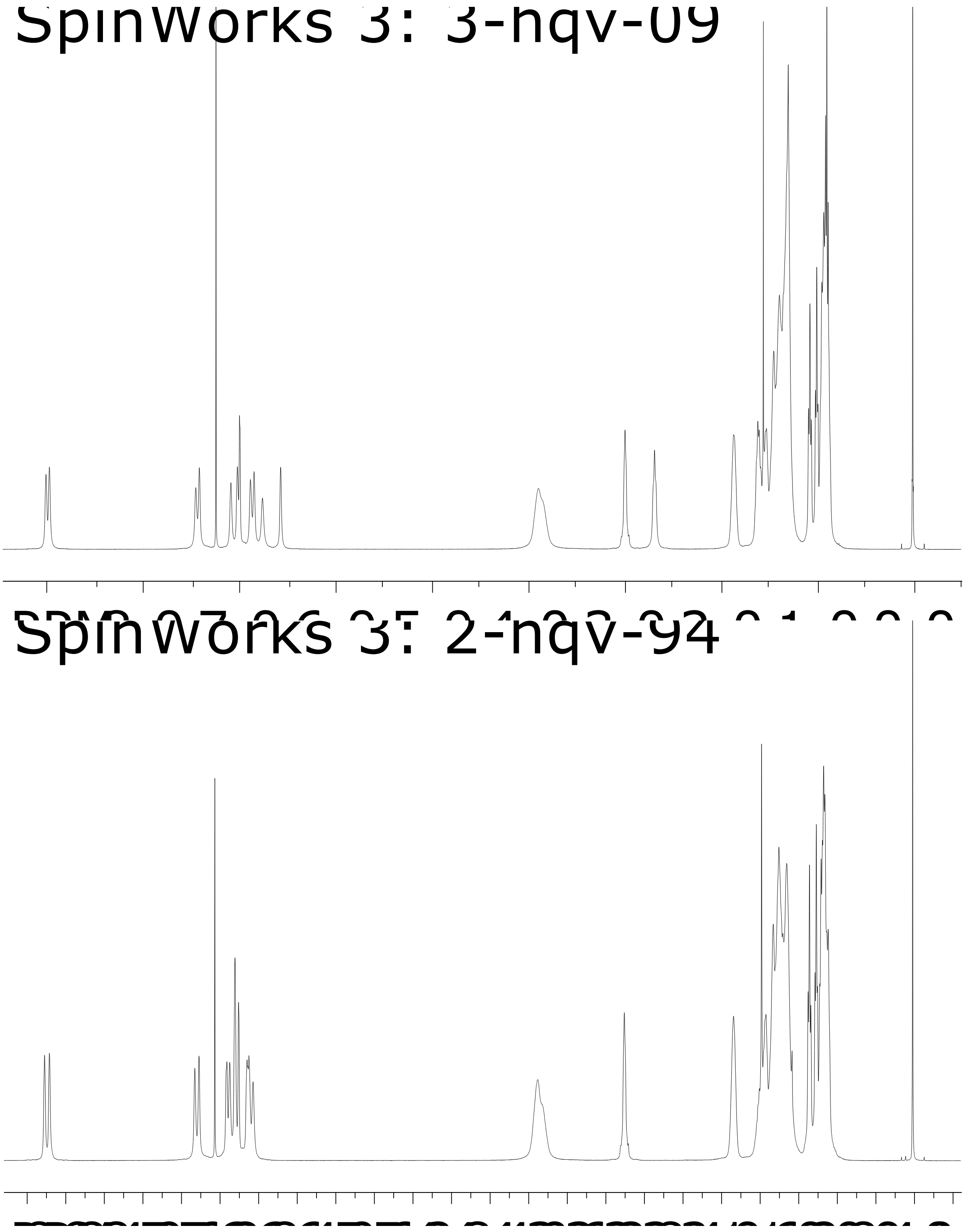

^{1}H NMR spectrum of **BDT(DPP-TTHex)$_2$** (top) and **BDT(DPP-TT)$_2$** (bottom)in $CDCl_3$ (δ 7.26 ppm).

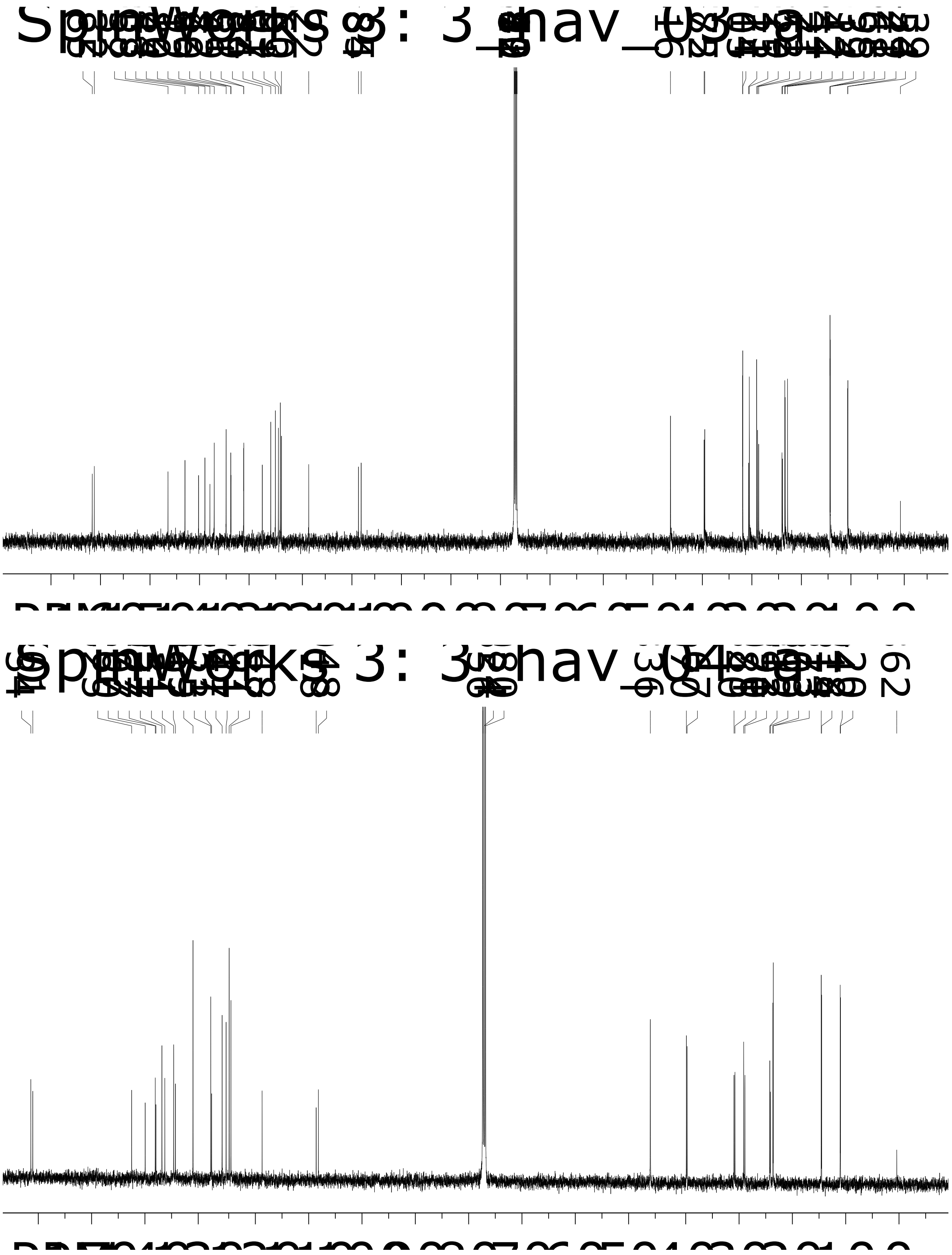

^{13}C NMR spectrum of compound **2a** (top) and **2b** (bottom) in CDCl$_3$

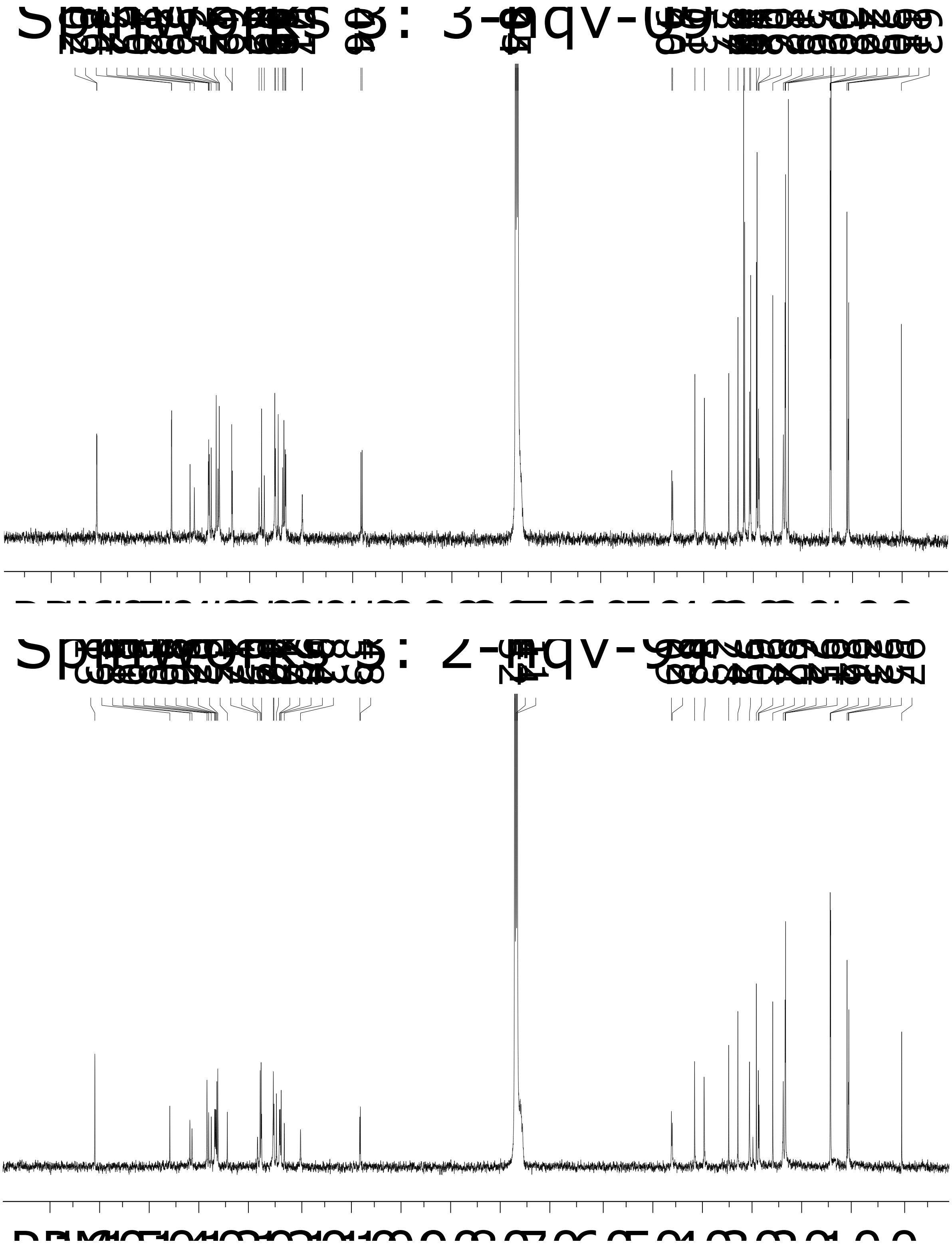

^{13}C NMR spectrum of compound **BDT(DPP-TTHex)$_2$** (top) and **BDT(DPP-TT)$_2$** (bottom) in $CDCl_3$

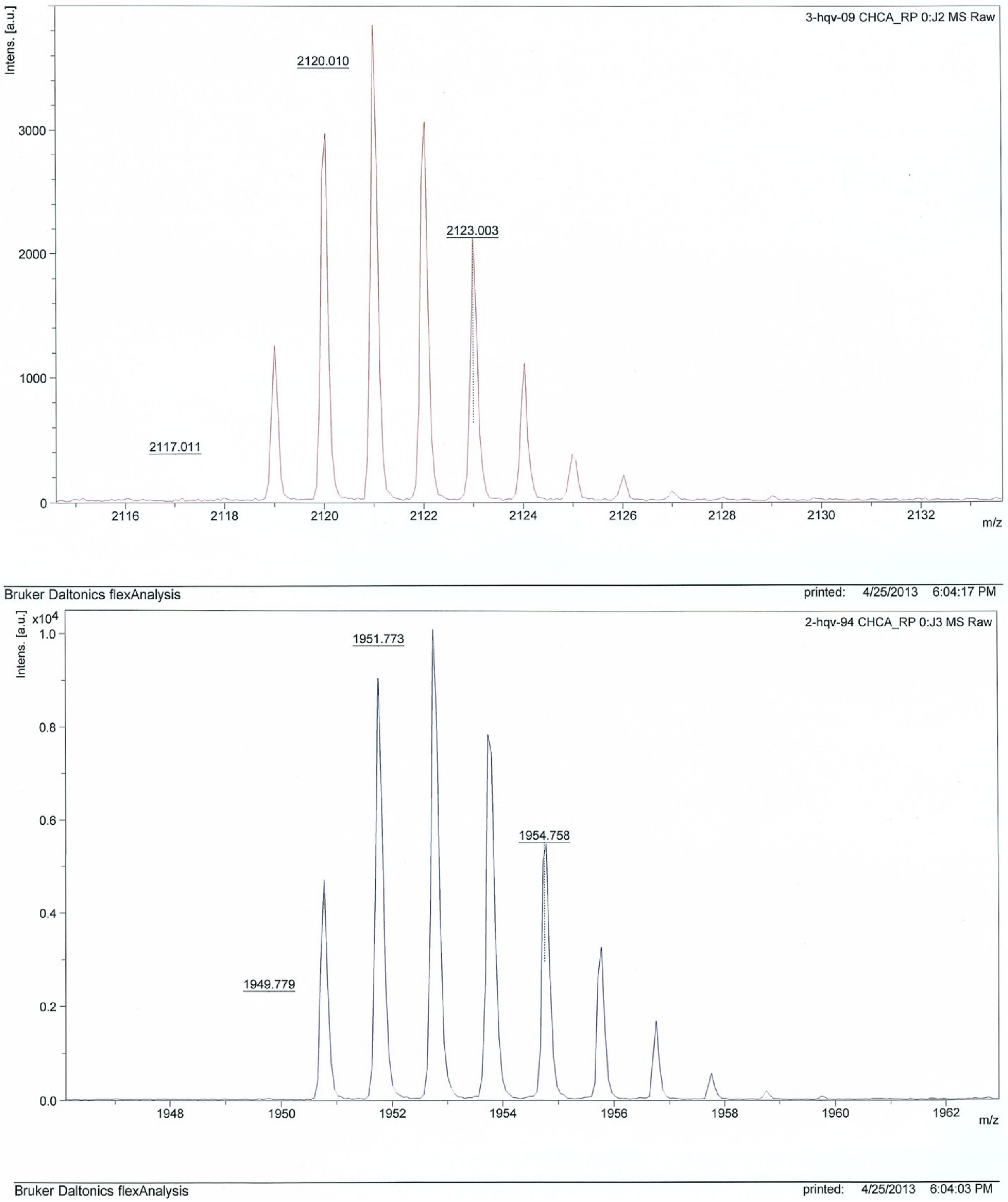

MS (MALDI-TOF) spectrums of BDT(DPP-TTHex)$_2$ (top) and BDT(DPP-TT)$_2$ (below)

Reference

1. L. Huo, S. Zhang, X. Guo, F. Xu, Y. Li and J. Hou, *Angew. Chem. Int. Ed.*, 2011, 50, 9697-9702.
2. L. Huo, J. Hou, H.-Y. Chen, S. Zhang, Y. Jiang, T. L. Chen and Y. Yang, *Macromolecules*, 2009, 42, 6564-6571.